EFDA–JET–PR(08)20

A.V. Krasilnikov, D. Van Eester, E. Lerche, J. Ongena, V.N. Amosov, T. Biewer, G. Bonheure, K. Crombe, G. Ericsson, B. Esposito, L. Giacomelli, C. Hellesen, A. Hjalmarsson, S. Jachmich, J. Kallne, Yu.A. Kaschuck, V. Kiptily, H. Leggate, J. Mailloux, D. Marocco, M.-L. Mayoral, S. Popovichev, M. Riva, M.Santala, M. Stamp, V. Vdovin, A. Walden and JET EFDA contributors

Fundamental Ion Cyclotron Resonance Heating of JET Deuterium Plasmas

Fundamental Ion Cyclotron Resonance Heating of JET Deuterium Plasmas

A.V. Krasilnikov[1], D. Van Eester[2], E. Lerche[2], J. Ongena[2], V.N. Amosov[1], T. Biewer[3], G. Bonheure[2], K.Crombe[4], G. Ericsson[5], B. Esposito[6], L. Giacomelli[5], C. Hellesen[5], A. Hjalmarsson[5], S. Jachmich[7], J. Kallne[8], Yu.A. Kaschuck[1], V. Kiptily[7], H.Leggate[7], J. Mailloux[7], D. Marocco[6], M.-L. Mayoral[7], S. Popovichev[7], M. Riva[6], M. Santala[9], M.Stamp[7], V.Vdovin[10], A.Walden[7] and JET EFDA contributors*

JET-EFDA, Culham Science Centre, OX14 3DB, Abingdon, UK

[1]SRC RF Troitsk Institute for Innovating and Fusion Research, Troitsk, Russia
[2]Laboratory for Plasma Physics – ERM/KMS, TEC partner, Brussels, Belgium
[3]Oak Ridge National Laboratory, Oak Ridge, TN 37831, USA
[4]Department of Applied Physics, Ghent University, Gent, Belgium
[5]Department Physics and Astronomy, Uppsala University, Uppsala, Sweden
[6]ENEA, Frascati, Italy
[7]EURATOM-UKAEA Fus. Assoc., Culham Science Center, United Kingdom
[8]Department Engineering Sciences, Uppsala University, Uppsala, Sweden
[9]VTT Technical Research Centre of Finland, Association EURATOM-Tekes, P.O.Box 1000, FIN-02044 VTT, Finland
[10]RNC Kurchatov Institute, Nuclear Fusion Institute, Moscow
** See annex of M.L. Watkins et al, "Overview of JET Results ", (Proc. 21 st IAEA Fusion Energy Conference, Chengdu, China (2006)).*

Preprint of Paper to be submitted for publication in
Plasma Physics and Controlled Fusion

ABSTRACT

Radio frequency heating of majority ions is of prime importance for understanding the basic role of auxiliary heating in the activated D-T phase of ITER. Majority Deuterium Ion-Cyclotron Resonance Heating (ICRH) experiments at the fundamental cyclotron frequency were performed in JET. In spite of the poor antenna coupling at the lowest possible commissioned RF frequency (25MHz), this heating scheme proved promising when adopted in combination with D Neutral Beam Injection (NBI). The experiments were performed in a ~90% D, 5% H plasma with some pulses including traces of Be and Ar. Up to 2MW of ICRH power was applied with dipole phasing in conjunction to ~6MW of NBI power, either using 80keV "normal" beam or 130keV "tangential" beam injection. The toroidal magnetic field strength was typically $B_0 = 3.3T$, providing core ICRH of the bulk D ions. The effect of fundamental D ICRH was clearly demonstrated in these experiments: By adding ~25% of heating power ($P_{ICRH} = 1.7MW$ / $P_{NBI+OH} = 7MW$) the fusion power was increased up to 30-50%, depending on the type of NBI adopted. At this power level, the ion and electron temperatures increased from $T_i \sim 4.0keV$ and $T_e \sim 4.5keV$ (NBI-only phase) to $T_i \sim 5.5keV$ and $T_e \sim 5.2keV$ (ICRH+NBI phase), respectively. The increase in the neutron yield was stronger when 80keV rather than 130keV Deuterons were injected in the plasma. It is shown that the neutron rate, the diamagnetic energy and the electron as well as ion temperature scale roughly linearly with the applied RF power. A synergistic effect of the combined use of ICRF and NBI heating was observed: (i) The number of neutron counts measured by the neutron camera during the combined ICRF+NBI phases of the discharges exceeded the sum of the individual counts of the NBI-only and ICRF-only phases; (ii) A substantial increase in the number of slowing-down beam ions was detected by the TOFOR spectrometer when ICRF power was switched-on; (iii) A small D subpopulation with energies slightly above the NBI launch energy were detected by the neutral particle analyzer and g-ray spectroscopy.

1. INTRODUCTION

A well known advantage of ion cyclotron resonance heating of plasmas in future fusion reactors, including ITER, is the dominant ion heating leading to higher Q gain and possibilities for efficient driven burn control. In most present-day tokamaks and stellarators, the standard plasma heating scenario is based on the resonant interaction of externally launched waves with a relatively small concentration of resonant ions that efficiently absorb ICRF power at their fundamental cyclotron frequency and redistribute this power collisionally due to the drag of the energetic minority tail both on the electrons and on the bulk ions. As this scheme depends on a minority gas being immersed in a bulk ion gas of a different species, this scheme of heating is usually referred to as "minority heating". It is this type of heating that will predominantly be used in ITER's non-activated hydrogen phase; D^+, $^3He^{2+}$ and $^4He^{2+}$ will be adopted as minority ions. One of these species, the $^3He^{2+}$ Helium isotope, will also be instrumental in enhancing the fusion yield in ITER's activated D-T phase, during which the concentration of the reacting deuterium and tritium populations will roughly be

balanced, necessitating a majority rather than a minority heating scheme. For this latter phase, it was proposed to adopt a wave absorption mechanism resting on finite ion Larmor radius effects: second harmonic heating of the bulk T ions. Since this harmonic of the tritons coincides with the fundamental cyclotron layer of the $^3He^{2+}$, the potential of majority T and minority $^3He^{2+}$ heating schemes can be combined to enhance fusion performance [1].

Second harmonic Tritium heating is currently the only RF heating scheme proposed for the main D-T ITER phase. Therefore, it seems worthwhile to examine the potential of supplementary (back-up) heating scenarios. As the first one that naturally comes to mind is a heating scheme that couples power to the second majority fuel ion species, D majority heating experiments were performed at JET.

Ion heating at the fundamental cyclotron frequency of the majority ions has been explored since decades, and even preceded the birth of minority heating schemes. There were successful experiments in the PPPL stellarator-C as early as 1968; the first Kharkov torsatrons and the US mirror traps date from that same era. In small tokamaks such as TM-1-Vch (1974) [2], TO-2 [3] in RRC "Kurchatov institute", T-11M [4] in SRC RF TRINITI and Globus-M [5] in the "Ioffe Institute" good heating results at the fundamental cyclotron frequency of the majority ions have also been reported. Furthermore, successful fundamental ICRH experiments were carried out in the L-2 stellarator [6]. Recently, the world's largest stellarator LHD - equipped with a vast set of diagnostics enabling to highlight various aspects of the dynamics of RF heated fast particle populations - has demonstrated bulk ion heating at the fundamental harmonic at high plasma densities close to those of scenarios foreseen for ITER's activated phase [7].

The experimental studies of majority Deuterium heating in JET envisaged approaching some of the ITER-like conditions. In view of its size, ITER can be operated both at higher density and temperature than what is possible in JET. Simulations predict the fundamental ICRF heating scheme to be more efficient on ITER than on current-day machines, exactly because of these higher densities and temperatures. But as it is impossible to simultaneously raise all the main plasma parameters to ITER-like values, this necessarily requires making compromises. The main characteristic of RF heating being its potential to create fast particle populations, it was decided for the experiments reported on in this paper to adopt deuterium neutral beam injection to create a subpopulation of fast D ions that approximately simulates the ITER ions on which the RF power will interact.

The aim of the present paper is to discuss the experimental findings of the recent majority D experiments in JET, while other joint papers focus on specific wave- or fast particle-related aspects; the interested reader is referred to these papers for details on the interpretation of the results: Lerche et al. studied the non-Maxwellian RF heated D beam populations observed in these heating experiments using a coupled wave + Fokker-Planck equation solver, providing a global discussion of the interaction of RF waves with non-thermal populations and addressing the connection to the data collected by specific diagnostics [8]. One of the main conclusions of his paper is that the signature of the non-Maxwellian populations is very different from that of thermal particles, and in

particular that the Doppler shifted ICRF absorption of the D beam ions is a key ingredient to understand the experimental observations. The papers by Vdovin et al. [9] and Van Eester et al. [10] add further details to the former discussion, focusing respectively on the RF wave propagation as well as impurity absorption, and on fast particle aspects in more detail.

One of the issues still to be resolved to ensure that steady state conditions can be reached in ITER is the question of the long term impact of impurities in the plasma. As Be plasma facing components will probably be used in ITER, it is expected that non-negligible amounts of Beryllium (~2%) will be present in ITER discharges. Argon is considered as one of the possible options for creating a radiative belt at the plasma edge, intended to prevent excessive power flow to the divertor. As far as RF heating is concerned, Be (Z/A = 4/9) and Ar (Z/A = 18/40) are almost D-like species, i.e., have their cyclotron layers near to that of the Deuterons. Hence, any Deuterium RF heating scheme is likely to be benefiting or suffering from parasitic impurity heating. Be and Ar traces were purposely added to the plasma in the majority D heating experiments to study these species' behavior under the influence of ICRH. Beryllium was evaporated in the machine prior to the experimental sessions and its initial concentration was estimated to be about 1.5%. Argon puffs were applied in a limited number of shots.

Apart from this introduction, the present paper comprises the following sections: The experimental arrangement is discussed in Section 2, while the main results of the D majority fundamental ion cyclotron heating experiments in JET are given in Section 3. A brief section on the outcome of modeling is reserved to Section 4, and conclusions are formulated in Section 5.

2. DESCRIPTION OF THE EXPERIMENTAL CONDITIONS

JET is routinely operated at magnetic field values of $B_0 \sim$ 3-3.5T. At these magnetic field values, central majority D heating requires ICRF antenna frequencies of f ~ 25MHz. The JET 4×4-strap A2 antennae are powered by generators that can be operated between 23 and 57MHz. Being primarily designed for heating at the higher frequencies (Hydrogen minority heating at 51MHz being the best performing heating scheme) the antenna coupling at 25MHz is typically poor. Moreover, since majority D heating is characterized by low single pass absorption for typical JET parameters, the RF system needed to be tuned carefully during the two experimental sessions to deliver as much as possible RF power under unfavorable conditions. The maximal ICRF power reached was 2MW. To optimize heating, dipole phasing was imposed; for this phasing the antenna current density spectrum peaks at approximately $|k_{||}| \approx 6.6\ m^{-1}$. Except for the natural level of Hydrogen typical of JET (~5%) and small traces of Ar and Be purposely introduced in some discharges, the plasmas were mainly composed by Deuterium ions in all reported experiments. The D population was primarily constituted of a low energy component (the thermalized bulk D ions) and of a sub-population of ~10% non-thermal D ions (neutral beam ions injected with initial energies of 80keV or 130keV depending on the discharge). The beam population serves a double purpose: (i) As ITER plasmas will be hotter than those of JET, the slowing down JET beam ions have some similar characteristics

(e.g. the collisionality) of the ITER bulk ions; (ii) But as instabilities are triggered by fast particle subpopulations, the beam particles also represent a seed pool for energetic particles potentially created through RF wave – particle interactions. Note that as the resonant interaction between the RF wave and the beam ions takes place at the Doppler-shifted cyclotron resonance $\omega = \omega_{cD} - k_{||} v_{||}$ (with w the generator frequency, ω_{cD} the D cyclotron frequency, $k_{||}$ the parallel wave number and $v_{||}$ the velocity component of the particle along the static magnetic field B_0) rather than at the "cold" resonance ($\omega = \omega_{cD}$), the dominant wave heating of the bulk D ions and the beam D ions typically occurs at different locations. Figure 1 gives a sketch of the cyclotron positions for various plasma species as function of the equilibrium magnetic field at $R_0 = 2.96$m for a generator frequency of f = 25MHz. The experiments were performed with $B_0 = 3.3$T and IP = 2MA. For that magnetic field strength, the thermal deuterons resonance layer is close to the plasma center ($R^a 3$m) while the Doppler-shift of e.g. a 130keV D ion is approximately 0.5m. Typical densities and temperatures were around $N_{e0} = 2.5 \times 10^{19}$ m^{-3} and $T_{e0} = T_{i0} = 5.0$keV in most pulses.

JET is equipped both with "normal" and with "tangential" beams. A first series of experiments was performed with 5MW of 80keV deuterium NBI injected from octant 4 (see Fig.2) at about ~800 to the magnetic axis ("normal" beam) and 1.3MW of 130keV beam injected at ~600 ("tangential" beam). A subsequent series adopted 6MW of the higher energy 130keV beam, integrally injected from octant 8 at ~600 to the magnetic axis ("tangential"). To allow a detailed study of the various ICRF absorption mechanisms expected in the experiments and their impact on the global plasma properties, all discharges contained a phase during which only NBI was present ($P_{NBI} \sim 6$MW), a phase during which RF and beam sources were active and an RF-only phase (with only ~1.5MW of diagnostic beam power needed to have ion temperature data). As ELMs and the associated changes in antenna loading commonly make analysis of the RF power deposition profile more difficult, and in view of the already limited amount of available RF power and the many trips of the generator under trying circumstances, the NBI power was purposely kept low so that the plasma remained in L-mode. To avoid sawteeth during the main phase of the experiment, the plasma current diffusion was delayed by applying ~1.7MW of lower hybrid heating at the beginning of the discharges.

Values of the electron temperature $T_e(r)$ and density $N_e(r)$ profiles are routinely provided at JET. The fast electron temperature diagnostic relies on Electron Cyclotron Emission (ECE) and provides the temperature on 96 positions across the plasma with a time resolution of typically 1.0-2.5kHz [11]. Various diagnostics provide local or line integrated information on the electron density. The density profile is usually inferred from the Thomson scattering (LIDAR) diagnostic providing the density at 50 radial positions with a time resolution of 250ms [12]. The bulk ion temperature $T_i(r)$, as well as the density and temperature of impurities such as C, Ar and Be are not routinely provided and require dedicated post-pulse-processing of charge exchange (CXRS) measurements [13]. A number of specialized diagnostics available at JET were exploited to examine the impact of the RF power on the plasma. Of particular interest were the horizontal "low energy" neutral particle analyzer KR2 [14], adjusted for charge exchange deuteron atom energy distribution measurements in the

range of 120 – 370keV, the perpendicular and tangential neutron compact spectrometers of NE-213 [15] and the Stilbene [16] detectors, the vertical neutron time-of-flight spectrometer TOFOR [17], the radial and vertical neutron cameras [18] and the γ-ray spectrometers [19].

3. RESULTS OF ICRH AT THE FUNDAMENTAL FREQUENCY OF THE MAJORITY DEUTERONS AT JET

In this section the main results of the experiments will be summarized. A more detailed discussion of the experimental results including a deeper interpretation of the interlinked features observed by the various diagnostics based on modeling of the wave-particle interaction lies outside the scope of this paper.

The time traces of the total neutron rate, the plasma stored diamagnetic energy (Wdia) and the central electron temperatures measured by Thomson scattering (LIDAR) and Electron-Cyclotron Emission (ECE) in Pulse No: 68287 are presented in Fig.3. The NBI and ICRH power levels applied to the plasma are also shown. Approximately 5MW of 80keV and 1.3MW of 130keV were applied in this discharge. The impact of the application of ~1.7MW of ICRF power is visible in almost all traces. In particular, the fusion power increases by ~45% when only ~25% of heating power is added by ICRF. Although part of this increase is due to the natural evolution of the plasma – a steady state not yet being reached when the RF power is switched on – about 35% of the fusion power increase is believed to be associated to ICRF heating in this pulse, both directly due to the RF power absorption of the thermal and fast beam deuterons and indirectly due to the increase in the electron temperature and consequent decrease in the plasma collisionality and change in the slowing-down time of the beam ions [8].

Considerable increases in the bulk species temperatures were also observed during the combined ICRF + NBI phases of various discharges. In Fig.4, the time evolution of the ion and the electron temperatures measured at several plasma radii by, respectively, the CXRS diagnostic (KS5) and the fast ECE radiometer (KK3) in Pulse No: 68733 are plotted together with the ICRF and NBI power levels applied. Around 6MW of 130keV tangential NBI was applied in this discharge. One clearly sees the response of the ion and electron temperature signals to the RF waveform. Temperature increases up to $\Delta T_i \approx 1$keV and $\Delta T_e \approx 0.5$keV are observed near the plasma center when adding ~1.7MW of RF power. Both electron and ion temperatures show a small decrease in the outer plasma region right after the ICRH start-up, an effect attributed to the enhanced impurity influx from the wall into the plasma. This effect, which is stronger in low single pass absorption scenarios, fades out after t~0.5s.

For practically all discharges, a systematic data analysis concerning the impact of different RF power levels on several plasma parameters was done. To increase the statistics and reduce the influence of the natural evolution of the discharge in the data analysis, the studied quantities were averaged over various time intervals ($\Delta t \sim 0.5$s) in each pulse and compared with their values in a time interval where $P_{RF} = 0$, corresponding to the NBI-only phase. The results of the changes in the

neutron yield, the diamagnetic energy as well as the central ion and electron temperature as function of the applied RF power level are summarized in Fig.5. The error bars represent the standard deviation of the data in the various time intervals considered.

First note that the RF power coupled to the plasma and consequently the neutron rate and the diamagnetic energy is gradually increased from shot to shot, achieving its maximum at the end of the pulse series presented (Pulse No: 68288). This stresses the need for dedicated tuning of the RF circuit during the session to successfully cope with the challenging conditions inherent of this (…) scenario. One clearly sees the improvement of the plasma performance with increasing RF power: the neutron rate increases from roughly 9×10^{14} to 14×10^{14} counts (~50%) and the stored energy from 1.3J to 1.75J (25%) when approximately 1.6MW of RF power is coupled to the plasma. Both quantities exhibit a nearly linear dependence on the RF power applied. It is important to mention that a considerable enhancement of the radiated power was observed during the application of ICRF in these experiments, a consequence of the rather poor single-pass absorption of the scenario. When subtracting the radiated power from the injected RF power to get the "effective" power applied to heat the plasma, the performance enhancement would be even more pronounced.

The slowing-down time depends on the temperature Te and density Ne of the bulk plasma in which a fast particle population is immersed: $\tau_s(s) = 0.133[A/Z^2]T_e(keV)^{3/2}/[N_e(10^{19}m^{-3})]$; A and Z are the mass and charge numbers of the examined population, respectively. Even when the source creating the particles is always the same, the fast particle density will be different if the bulk plasma characteristics are changed. In Fig.6, the slowing-down time inferred from the values of the central electron temperature and density averaged during several time intervals of a series of discharges is represented as function of the ICRF power applied. Despite the somewhat large error bars related to the LIDAR density measurements, there is a noticeable correlation between the applied RF power and the slowing down time: the higher the RF power level, the longer it takes for fast beam particles to slow down. The slowing down time changes from about $\tau_s = 0.9$s in the (6MW) NBI-only phase of the discharge to $\tau_s \approx 1.1$s when ~2MW of ICRF power is also applied. One expects such a change to be noticeable in experimental findings of diagnostics that depend on the supra-thermal particle density. Such an increase of the fast particle density was indeed noticed by various neutron and fast particle diagnostics, as will be discussed later.

Although the importance of the ICRF-NBI synergism is clear for the D majority experiments reported here (see [8] for an example of the interaction between the beam ions and the RF wave fields), a more in depth study of the impact of the RF power on different beam sources still needs to be made. One striking aspect is depicted in Fig.7, which shows the relative increase of the neutron rate as a function of the RF power density for different NBI populations. In absence of RF, the neutron count is about 9×10^{14} for the 80keV and 12×10^{14} counts for the 130keV beams. Both the data points of the 80keV beam and the 130keV beam show that the neutron rate increases with RF power, an effect that can be anticipated since the underlying D-D fusion reaction rate is an increasing function of the D energy in the relevant energy range. The same logic would, however, lead to the

conclusion that for a given amount of RF power absorbed by the beam ions, the relative increase in the neutron yield for the 130keV beam case should be higher than the increase for the 80keV case. The results in Fig.7 clearly show that the opposite is the case: the 80keV NBI data points systematically lie higher than those of the 130keV beam. At $P_{RF} \approx 1.7$MW the relative increase of the neutron rate associated with the 80keV beams is roughly twice the increase found for the 130keV beams. The fact that the slope of the neutron count increase as a function of RF power is steeper for the slower beam particles suggests that the ICRF-NBI interaction can not be interpreted by simple intuitive arguments, but that it rather depends on a delicate balance between the characteristic slowing-down dynamics of the beam ions and the Doppler-shifted ICRF acceleration of these ions, which is strongly dependent on the spatial structure of the RF fields generated in the plasma. A more detailed analysis is obviously required to explain this observation.

The change of the vertical and horizontal neutron camera signals during the different heating phases (NBI-only, ICRF + NBI and RF-only) of Pulse No: 68288 is illustrated in Fig.8. The signals were integrated during a 100ms time window in each phase. Note the synergistic effect: The neutron yield measured during the combined ICRF + NBI phase exceeds the sum of the individual counts obtained in the RF-only and the NBI-only phases in all channels, suggesting that the slowing-down time of the NBI ions is indeed increased during the application of ICRF power.

The effect of ICRF wave interaction with the injected deuteron beam was also noticed in the horizontal NPA measurements. This diagnostic measures the energy distributions of CX deuterium atoms leaving the plasma perpendicular to the magnetic axis in the equatorial plane. In Fig.9, the energy distributions of the fast deuterons obtained during the NBI-only, the ICRF + NBI and the RF-only phases of Pulse No: 68733 are compared. During the combined ICRF + NBI phase a small subpopulation of beam deuterons is accelerated to energies exceeding that of the beam injection energy. Although relatively modest, the magnitude of this energy change increases with ICRH power, reaching approximately 180keV for $P_{RF} = 1.7$MW. The effective perpendicular temperature of the fast deuterons was estimated to reach ~ 50keV during the combined ICRF+NBI phase under these conditions.

Although not clearly evident in the NPA results (the chosen settings for the diagnostic made that the minimum energy of the fast deuteron measurements was only slightly below the maximum beam source energy), a main effect of the RF power absorption in the experiments is the increase in the population of slowing-down NBI ions at and below the beam injection energy. These ions (rather than the faster ions detected by the NPA) are believed to be mostly responsible for the enhanced D-D fusion yield observed during the combined application of NBI and ICRH power. This is confirmed by measurements performed with the neutron spectrometer TOFOR, which detected roughly twice as much 2.5MeV neutrons (from D-D reactions) in the combined NBI + ICRF phase of Pulse No: 68288 than in the NBI only phase, as depicted in see Fig.10. Modeling of the neutron spectra using trial distribution functions for the various D populations (thermal, beam and fast) shows that the main contribution to the increase in the neutron count detected by TOFOR

comes indeed from deuterons with energies below the beam source energy. Practically no indication of a high energy tail formation was found in the TOFOR analysis, confirming that the RF induced D tail detected by the NPA diagnostics is indeed very small. However, as the “low” energy NPA has a horizontal line-of-sight close to the plasma mid-plane and TOFOR “sees” the plasma core along a vertical cone, these diagnostics may detect different features of the same particle distribution [8]. The compact neutron spectrometers, NE-213 (with vertical line-of-sight) and the Stilbene (with tangential view) also did not detect any major changes in the shape of the D-D neutron energy distribution due to ICRH. In agreement with the TOFOR results, it was found that the distribution of the deuterons in the 5-100keV supra-thermal energy range is mostly determined by slowing down of fast beam deuterons, which, due to the ICRH power absorption, have their slowing-down time increased leading to a higher D-D fusion yield.

All these observations are in qualitative agreement with the ~20% increase in the slowing-down time inferred from the electron temperature and density changes observed when ca. 2MW of RF power is applied to the plasma (see Fig. 6).

To compare the relative efficiency of on- versus off-axis majority D heating as well as the role of ICRF impurity absorption in JET, Pulse No: 68734 was done at a higher magnetic field; $B_0 = 3.6$T instead of the otherwise used field strength $B_0 = 3.3$T. As shown in Fig.1, the ICRF resonance layers moved as follows: for plasma deuterons from R = 3.0m (on-axis) to R = 3.27m (off-axis), for Be and Ar impurities from R = 2.69m and R = 2.72m (off-axis) to R = 2.96m and R = 2.99m (on-axis). As can be seen in Fig.11, despite the different B_0 and the slight different ICRF waveform, the main parameters of Pulse No’s: 68733 and 68734 are very similar for what concerns (a) ICRH and NBI power, (b) central electron density, (c) central electron temperature (d) diamagnetic energy and (e) total neutron rate. However, hints on differences in the ion (CXRS) and electron (KK1) temperature profiles were observed, as depicted in Figs.11 (f) and (g), respectively. The electron profile, in particular, seems to be somewhat broader in the central region of the plasma for the higher B0 pulse. No convincing differences in the NPA atomic spectra or in the neutron spectrometer measurements were noticed at the available power levels. Since only one pulse was performed at $B_0 = 3.6$T, further experimenting is required to reach firmer conclusions about possible differences in the heating efficiency due to the slightly distinct ICRH conditions.

As there were no means to directly inject Be during the discharges themselves, it was evaporated into the machine the night before the experiment. The effect of the evaporation died away quickly after a few shots, as was clearly observed by visible spectroscopy (see Fig.12a). It was impossible to infer a reliable guess of the actual Beryllium concentration attained, but the maximal concentration was estimated to be around 1% in the earliest Pulse No: 68282. The effect of the Be concentration on the evolution of the power radiated by the plasma when 6MW of NBI is switched-on can be seen in Fig.12b: once the NBI heating is switched on, the intensity of the Be line emission and the radiated power increase, reaching a “steady state” after about 0.7s. Both the maximal level and particularly the slope of the radiated power growth after the NBI switch-on are gradually decreasing

shot after shot, roughly proportionally to the Be concentration. No firm evidence was found for RF heating of the Be impurity. This may be due to the fact that central RF heating of the fully stripped Be would require B_0 = 3.6T, and Be had been pumped out of the machine by the time the high field shot was performed.

There may though be evidences regarding the effect of RF heating on Argon: for identical Ar puffs bringing the Ar concentration to maximally ~0.5% in the RF heated phase of two subsequent plasma discharges, one at B_0 = 3.3T (ensuring central RF bulk D heating) and the other at 3.6T (ensuring central impurity heating), the effect of the Argon injection on the radiated power signal disappeared markedly slower for the on-axis impurity heating shot than for the other shot (Fig.13b). Although a small difference in the evolution of the line integrated density of these two discharges was observed (Fig.13c), this effect is still present when removing the density dependence from the bolometer signals (Fig.13d). Unfortunately, the RF generator tripped in Pulse No: 68733 approximately 0.5s after the Ar puff causing a decrease of ~0.4MW in the RF power level, making a quantitative comparative analysis of the radiation decay times hard. Moreover, since the impurity transport is very sensitive to the plasma characteristics [20], it is difficult to state if the different Ar behavior observed between Pulse No's: 68733 and 68734 is indeed due to the different ICRF conditions or due to the slightly different temperature profiles measured in these discharges (see Fig.11). Clearly more data need to be collected before any firm conclusions can be drawn in this respect.

4. NUMERICAL MODELING OF JET ICRH AT THE FUNDAMENTAL CYCLOTRON FREQUENCY: MAIN RESULTS

Intensive modeling was carried out for JET experimental conditions before, during and after the experiments. This detailed analysis is presented elsewhere (see [8], [9] and [10]) but some basic results are provided here. All simulations were performed for similar plasma content: 90-95% majority D (thermal + beam) ions, ~5% H and traces of Be, C and Ar. Other parameters used in simulations were the following: central density $N_e = 2.5\times10^{19}$ m^{-3}, central temperature $T_e = T_i$ = 5.5keV, magnetic field strength on axis B_0 = 3.3T and B_0 = 3.6T, neutral beam power P_{NBI} = 5 MW and energy E_{NBI} = 130keV, ICRH power P_{ICRH} = 2MW, RF frequency f_{ICRH} = 25MHz and dipole phasing (N = +27).

Typical distributions of the power absorbed by the various plasma constituents calculated taking into account the fast perpendicular injected beam deuterons are depicted in Fig.14. These results were obtained adopting the three-dimensional full wave code PSTELION [21]. In this code, the fast beam deuterons were described by a Maxwellian distribution with an effective temperature of 52keV shifted in the $v_{||}$-direction in velocity space. As a consequence of the position of the fast wave cut-off, fast deuterons having a Doppler shift of the resonance layer position towards the low field side are absorbing the ICRF wave power more efficiently than those having a Doppler shift towards the high field side.

To get an idea of the heating efficiency of an ICRH scenario, it is useful to determine its single

pass absorption rate. Since by definition all power launched from the antenna is ultimately absorbed inside the metallic vessel, 2D or 3D wave codes do not allow determining this quantity. Using the 1D TOMCAT code (which excludes the antenna region and yields the deposition profile but also the connection coefficients of all outgoing waves for a given incoming wave power) [22] it was found that the plasma only absorbs 5% of the power in a double transit over the plasma in absence of beams. This efficiency is roughly tripled (to a still modest 15%) when the preheating due to the beams is accounted for via a Maxwellian mock-up of the slowing down beam population. The low absorption efficiency suggests that large electric fields – particularly in the edge - are likely to be set up in this scenario and hence that interaction with the wall can be expected to be significant. This was indeed confirmed in the experiments via the increase of the plasma density, Z_{eff} and radiated power observed when RF power was applied.

The two-dimensional CYRANO [23] code was also used to study the fate of the RF power in the fundamental D ICRH scheme close to the experimental conditions mentioned above, taking into account the RF wave absorption by the fast NBI deuterons, modeled with the quasi-linear Fokker-Planck code BATCH [24]. The results show that the D beam ions play a crucial role in this RF heating scenario [8]: because their Doppler-shifted ion-cyclotron resonance lies far off-axis, they are more efficiently heated than the thermal (bulk) deuterons, whose power absorption suffers from the adverse polarization of the E_+ component of the RF electric field near the cold ion cyclotron resonance in the plasma center. When accounting for the actual beam distribution in the wave equation, it was shows that the beam ions have a maximum power absorption as far as 0.5m off-axis under conditions intended to favor core D bulk heating. With only ~8% of fast D beam ions in the plasma, roughly half of the total RF power applied is absorbed by the D beam ions, leading to the creation of a small sub-population of deuterons beyond the source energy and a substantial increase in the number of slowing down beam ions, in qualitative agreement with the experimental observations.

CONCLUSION AND FINAL REMARKS

Results on experiments aiming at ICRF heating of D majority plasmas at the fundamental cyclotron frequency performed in JET were presented. It was shown that the efficiency of this heating scheme is markedly increased when D neutral beams are used in conjunction with the RF waves. Even at the reduced power levels available at JET's lowest possible operating RF frequency, f = 25MHz, clear evidence of heating and enhanced performance was observed. No confinement degradation was seen during ICRH at the available RF power levels.

After proper tuning of the ICRF system to optimally cope with the low antenna coupling at 25MHz and the rather poor absorbtivity of this heating scenario, up to ~2MW of ICRF power was coupled to the plasma. This caused the electron and ion temperatures to increase by approximately $\Delta T_e \approx 0.7$keV and $\Delta T_i \approx 1.5$keV, respectively. By adding ~25% of heating power to the discharge ($P_{ICRH} = 1.7$MW / $P_{NBI + OH} = 7$MW) the D-D fusion power was increased by 30-50%, depending on

the type of neutral beam injection adopted. Contrary to simple intuition, the neutron yield increase due to ICRF heating is larger for 80keV than it is for 130keV beams. The total neutron yield as well as the diamagnetic energy and the central electron and ion temperatures scale roughly linearly with the applied RF power in the studied range.

A synergistic effect between NBI and ICRH was clearly observed: The neutron yield measured during the combined NBI+ICRF phases of the experiments exceeds the sum of the individual counts obtained in the RF-only and the NBI-only phases. This synergy is likely to result from the fact that the beam injected fast deuterons, because of their higher Doppler-shifts, absorb the ICRF power more efficiently than the thermal deuterons, which suffer from the characteristic adverse polarization of the RF electric fields near the cold cyclotron resonance layer of the majority ions (see [8] for details). The RF absorption of the NBI ions causes an increase in their slowing down time leading to an enhancement in the D-D reactions and therefore higher neutron emission. This is consistent with the observed modification of the slowing down time estimated from the changes in the electron temperature and density when ICRH is switched-on.

This effect is further confirmed by other neutron diagnostics, particularly by the neutron spectrometer TOFOR, which detects a substantial increase in the population of slowing-down beam ions when ICRF power is applied on top of NBI. The creation of a modest RF heated tail was observed by NPA in the energy range 120-200keV and was also noticed by γ-ray spectroscopy. Since the number of deuterons detected above the NBI injection energy is small, it is believed that the increased population of slowing-down deuterons is rather responsible for the enhanced neutron yield observed during the combined NBI+ICRH phases of the experiments.

The experiments provided hints that RF heating has a direct impact on impurities such as Ar and Be – which have similar charge to mass ratio than Deuterium and therefore were resonant in the fundamental D ICRH scenario - but prevented drawing firm conclusions on this point.

In spite of its advantages, the majority D heating scheme is – at the typical JET parameters and at the available frequency providing central D bulk heating – suffering from its low absorption efficiency, leading to enhanced impurity injection and increased Z_{eff} when RF power is switched on. This is likely due to the marginal single-pass absorption at the rather low plasma temperatures and densities adopted in the experiments that lead to large electric fields, in particular near the edge, and consequent enhanced plasma-wall interaction.

The present experiments – designed to position the cold D cyclotron resonance in the core region of the plasma – also suffered from the poor coupling of the ICRF heating system at 25MHz, which was designed to optimally couple power at higher frequencies. The role of the Doppler-shifted ICRF absorption of the D beam particles now being better understood (see [8] for details), it would be worthwhile to repeat the experiments at higher RF frequencies (29MHz or even 33MHz), at which more RF power can be coupled in the plasma and at which the ion cyclotron resonance layer of the NBI ions lies more central.

ACKNOWLEDGEMENT

This work was carried out within the framework of the European Fusion Development Agreement and the bilateral EU - Russion Federation agreement. The views and opinions expressed herein do not necessarily reflect those of the European Commission.

REFERENCES

[1]. D. Van Eester et al., Nucl.Fusion **42** (2002) 310–328.

[2]. V. Vdovin et al., "ICRH at fundamental frequency on TM-1-Vch tokamak" at IAEA Plasma Phys. and Contr. Fusion Conference 1974 (Tokyo).

[3]. L.I. Artemenkov, I.A. Kovan, I.A. Monakhov et al.. "Plasma heating at fundamental ion cyclotron frequency in the TO-2 tokamak", Plasma Physics and Controlled Nuclear Fusion Research, 1984, Proc. 10th IAEA Int. Conf., London, 12-19 Sept. 1984, IAEA, Vienna, 1985, Vol.1, p.615-621) see also: Amosov V.N. Artemenkov L.I., Kovan I.A., et.al., Sov.J. Plasma Physics, **14** (5), 363 (1988).

[4]. S.G. Maltsev, I.A. Kovan et.al., "Fundamental ICRH of T-11M hydrogen plasma" in Proceedings of 20-IAEA Fusion Energy Conference (2004), see also: N.B. Rodionov, E.A. Azizov, A.V. Krasilnikov et al., Sov. J. Plasma Physics, **32** (2), 1-11 (2006).

[5]. V.K. Gusev et al., "ICRF experiments on the spherical tokamak Globus-M" in Proceedings of 20-IAEA Fusion Energy Conference (2004).

[6]. V.A. Batyuk et al. in Controlled Fusion and Plasma Physics (Proc.11th Europ. Conf. Aachen, 1983) **7D**-1, 373, see also V.A. Batyuk et al., Sov. J. Plasma Phys. 1987, **13** (3), 143-148.

[7]. T. Mutoh, R. Kumazawa, T. Seki et al., Nucl.Fusion **43**, 738-743 (2003).

[8]. E.A. Lerche "D majority heating in JET plasmas: ICRH modeling and experimental RF power absorption", this special PPCF issue.

[9]. V. Vdovin et al., "……", in preparation.

[10]. D. Van Eester et al.,""JET (^{3}He)-D scenarios relying on RF heating: Survey of selected recent experiments", this special PPCF issue.

[11]. E. de la Luna et al., Rev. Sci. Instrum. **75**, 3831-3 (2004).

[12]. C. Gowers et al., "High Resolution Thomson Scattering on JET– an Assessment of the Feasibility", Report EFDA-JET-PR(01)29.

[13]. M.G. von Hellermann, Rev. Sci. Instrum. **61**, 3479-3486 (1990).

[14]. A.A. Korotkov et al., Nuclear Fusion **37**, 35-51 (1997).

[15]. L. Bertalot et al., Report EFDA-JET CP(05)-02-17 (2005).

[16]. Y.A. Kaschuck et al., Report EFDA–JET–CP(04)03-27.

[17]. A. Hjalmarsson et al., Rev. Sci. Inst. **74**, 1750-1752 (2003) and J. Kallne et al., "Advanced Neutron Diagnostics for ITER Fusion Experiments", 2—4, Report EFDA-JET-CP(04)07-19.

[18]. J.M. Adams et al., Nuclear Instruments and Methods in Physics Research **A329**, 277- 290 (1993).

[19]. V. Kiptily et al., Nuclear Fusion **42,** 999-1007 (2002).

[20]. M. Valisa et al., "Effect of radio-frequency power injection on impurity profile in JET plasmas", 49th Annual Meeting of the Division of Plasma Physics (DPP), Orlando, USA, November 2007.

[21]. V.L. Vdovin ICRF benchmarking modelling of ITER scenario #2, 7th Steady State Operation ITPA Topical Group meeting, Como, Italy, May 4-6, 2005.

[22]. D. Van Eester and R. Koch, Plasma Phys. Contr. Fusion **40**, 1949-1975 (1998).

[23]. P.U. Lamalle, "Nonlocal theoretical generalisation and tridimensional numerical study of the coupling of an ICRH antenna to a tokamak plasma", PhD thesis, Université de Mons, 1994 and LPP-ERM/KMS Report nr. 101.

[24]. D. Van Eester, Journal of Plasma Physics **65**, 407-452 (2001).

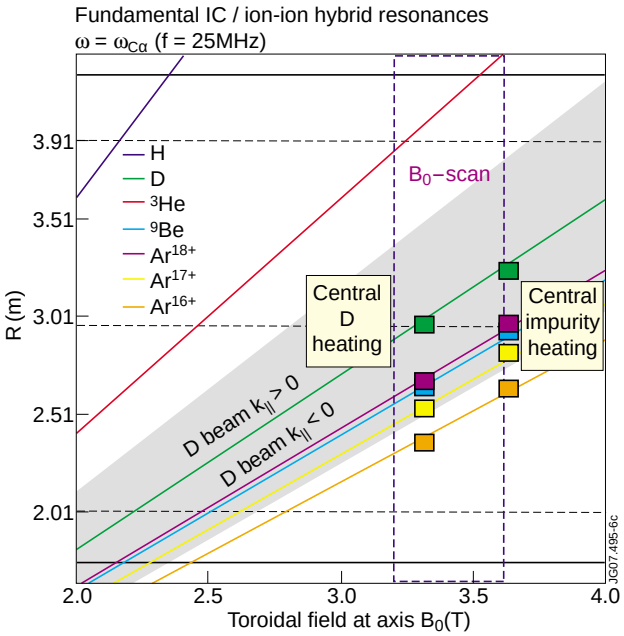

Figure 1: Dependence of the fundamental ion cyclotron resonance position on the axial magnetic field for various JET plasma ions.

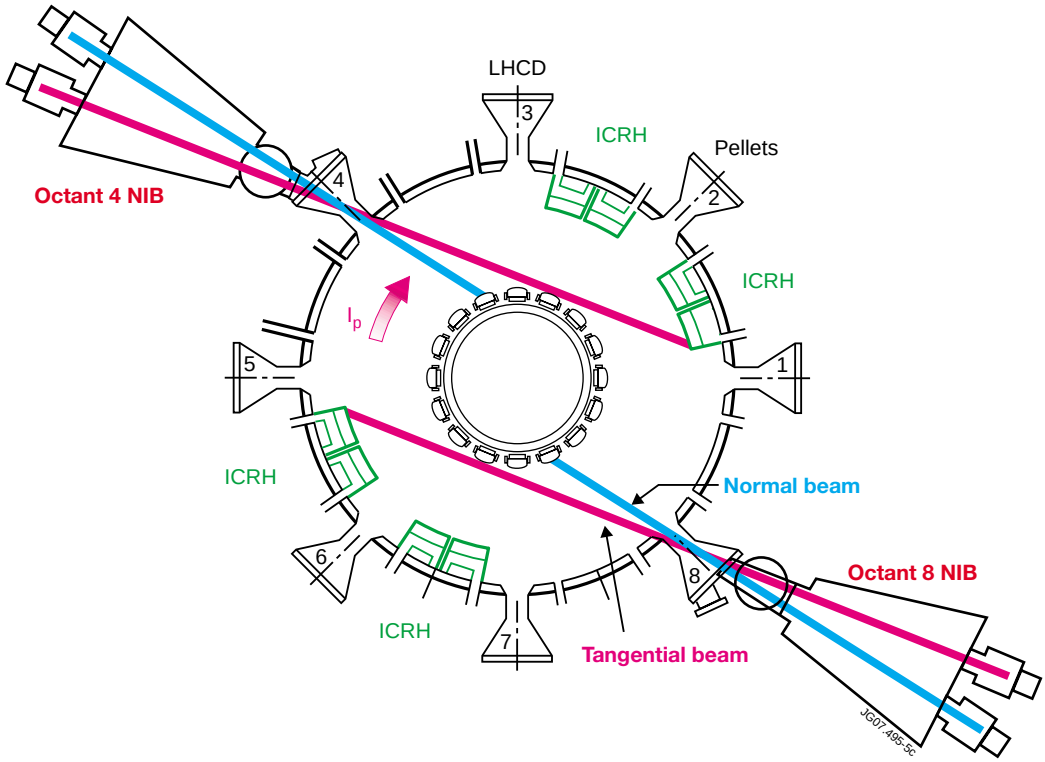

Figure 2: Arrangement of NBI and ICRH antennas at JET.

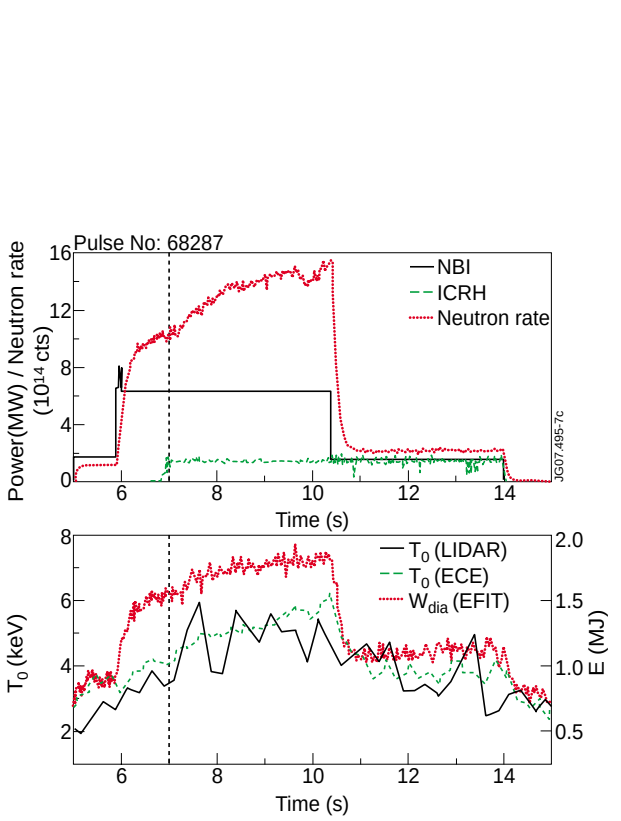

Figure 3: Evolutions of neutron rate, plasma stored energy (W_{dia}) and central electron temperature (T_0) together with NBI and ICRH powers in Pulse No: 68287.

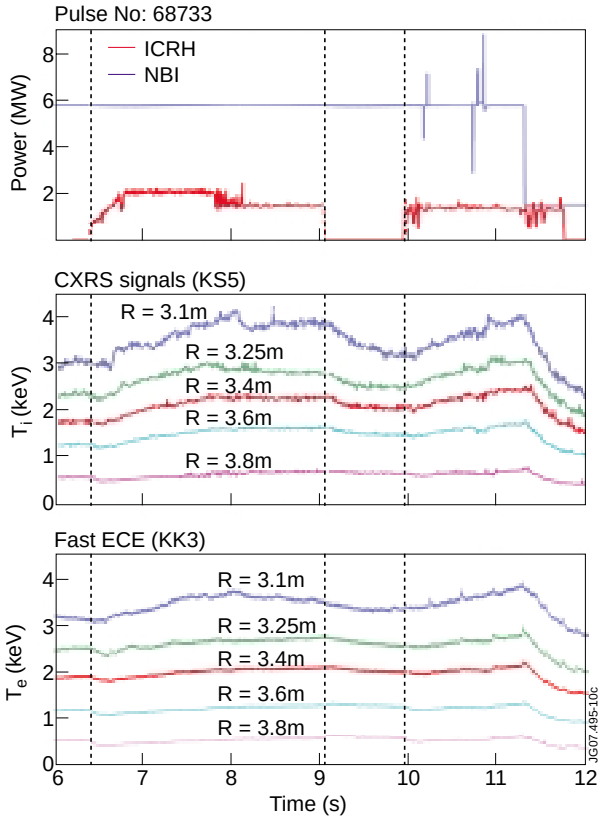

Figure 4: Evolution of the ion and electron temperature measured by the CXRS and ECE diagnostics, respectively, for several major radii ranging from 3.1 to 3.8m, plotted with NBI and ICRH power in Pulse No: 68733. At t=7s, the magnetic axis is at 2.97m. It shifts slightly more outward towards the end of the shot.

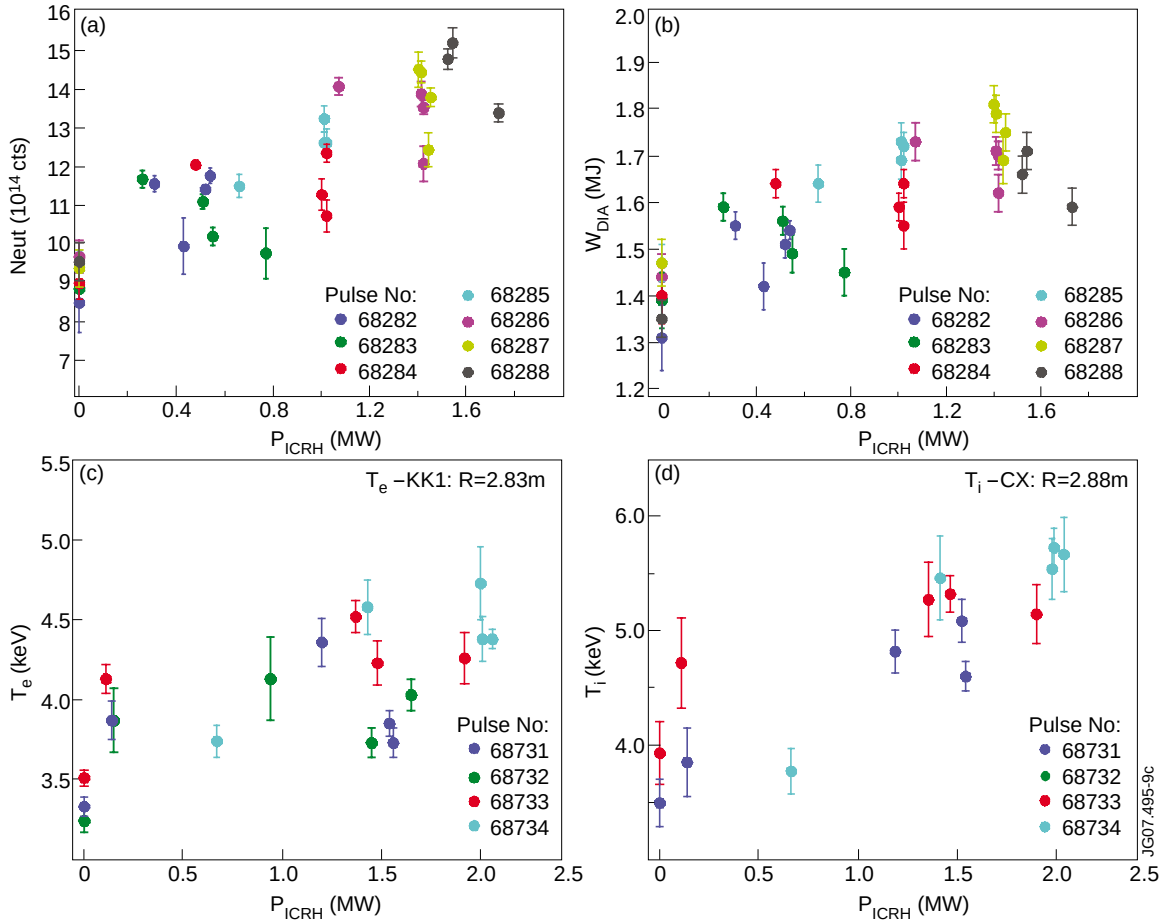

Figure 5: Total neutron yield (a), diamagnetic energy (b), central electron temperature (c) and central ion temperature (d) for Pulse No's: 68282-68288.

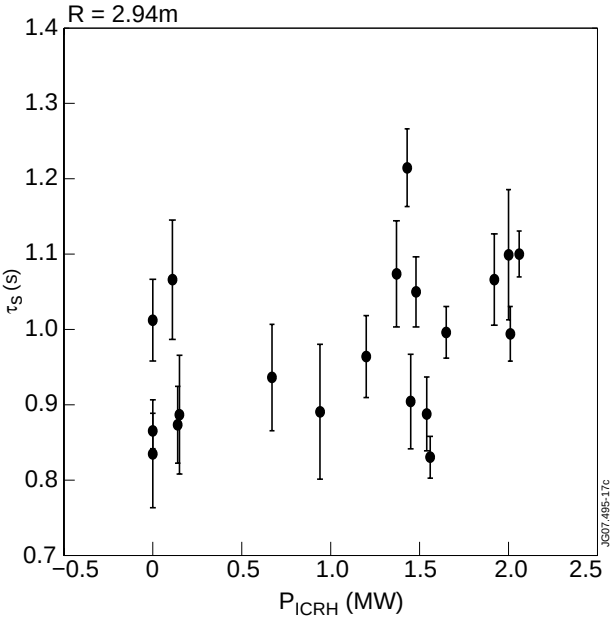

Figure 6: Fast deuteron slowing down time as a function of the ICRH power.

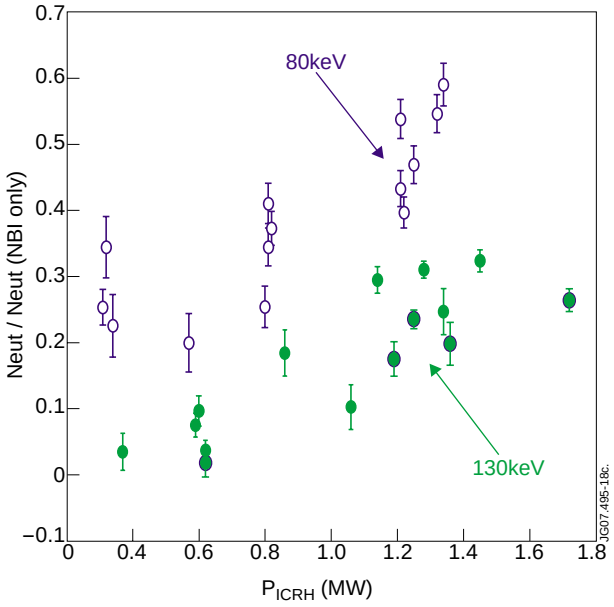

Figure 7: Relative neutron rate as a function of the RF power applied to plasmas preheated by NBI: (o) 5MW at 80keV + 1.3MW at 130keV "normal" NBI; (•) 6MW 130keV "tangential NBI".

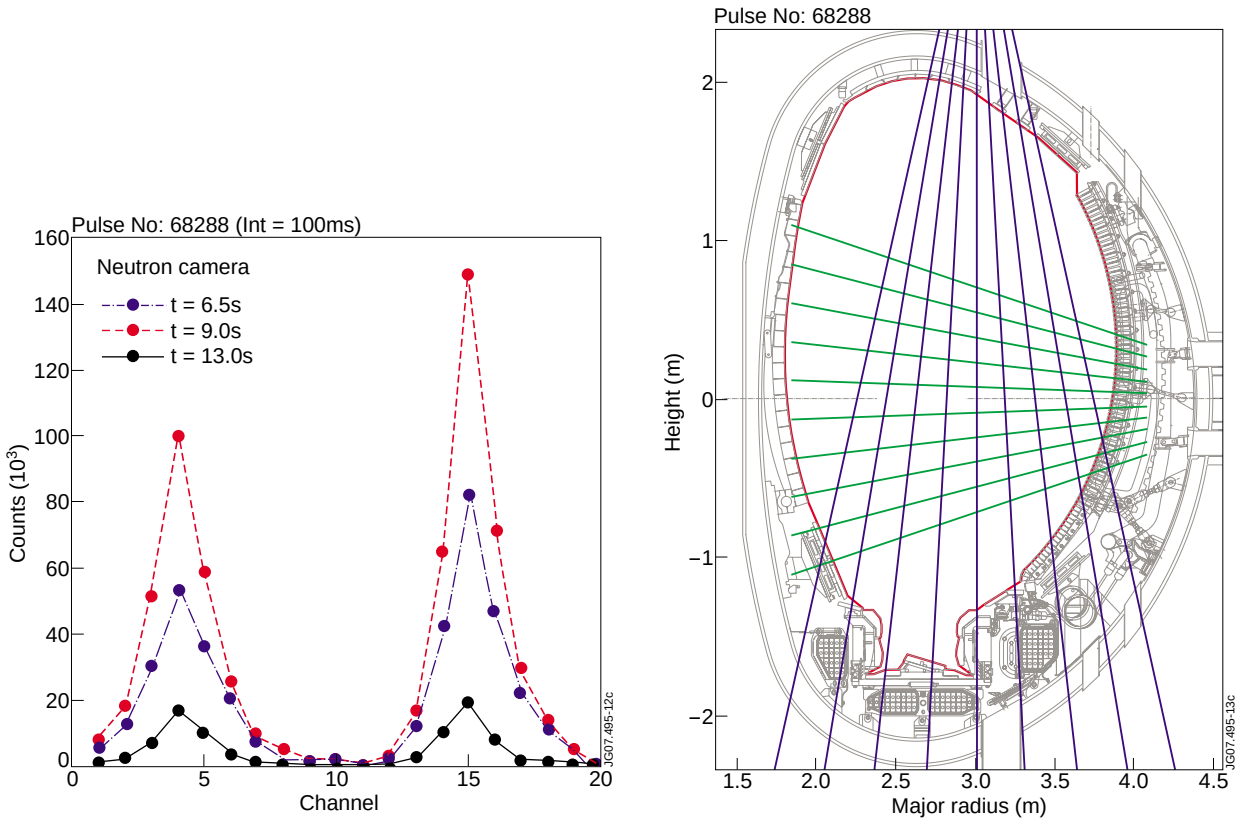

Figure 8: Neutron counts detected by horizontal (channel 1-10 from top to bottom) and vertical (11-19 from inward to outward) neutron cameras during Pulse No: 68288: neutron source profiles for time windows with 5MW perpendicular and 1.3MW tangential NBI (blue dash-dotted curve), same NBI together with 1.65MW ICRH (red dashed curve) and 1.3MW tangential NBI together with 1.65MW ICRH (black solid curve). The lines of sight of the neutron camera are provided in the figure on the right.

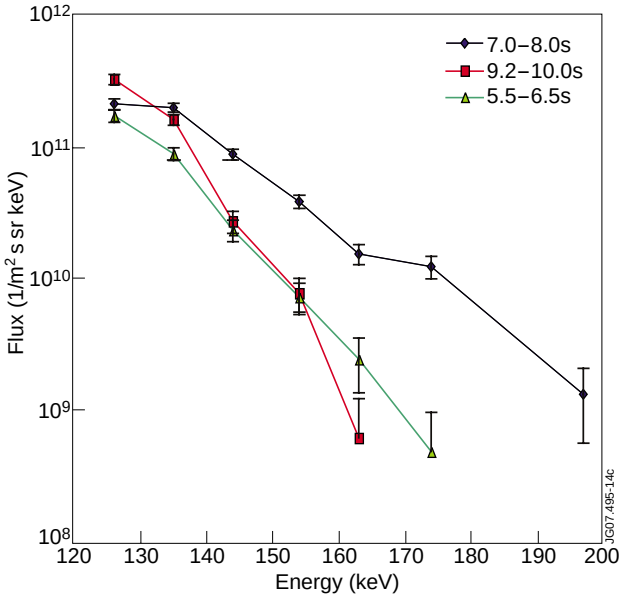

Figure 9: Perpendicular CX deuterium atom spectra measured by NPA during the NBI-only phases [5.5-6.5s] and [9.2-10.0s], and during the combined NBI+ICRH phase [7.0-8.0s] of Pulse No: 68733. In this pulse, 5.9MW of tangential 130keV beams and 2MW of RF power were applied.

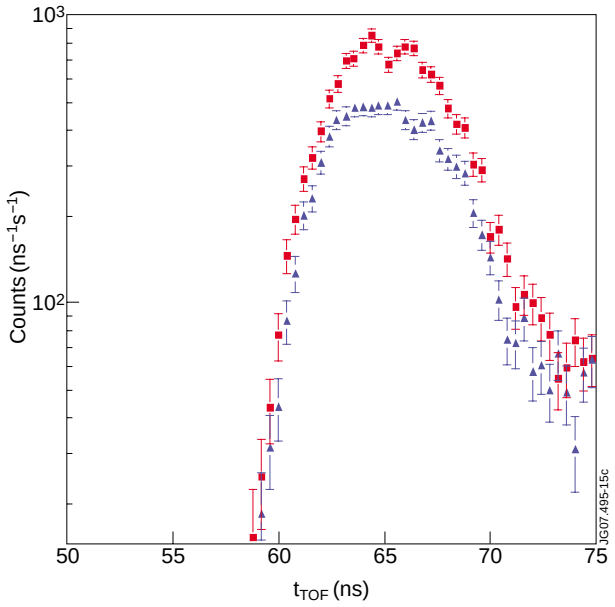

Figure 10: Neutron counts from D-D reactions (~2.5MeV) as function of time-of-flight measured with the neutron spectrometer TOFOR in two phases of Pulse No: 68288: (triangles) NBI-only, (squares) combined ICRF+NBI.

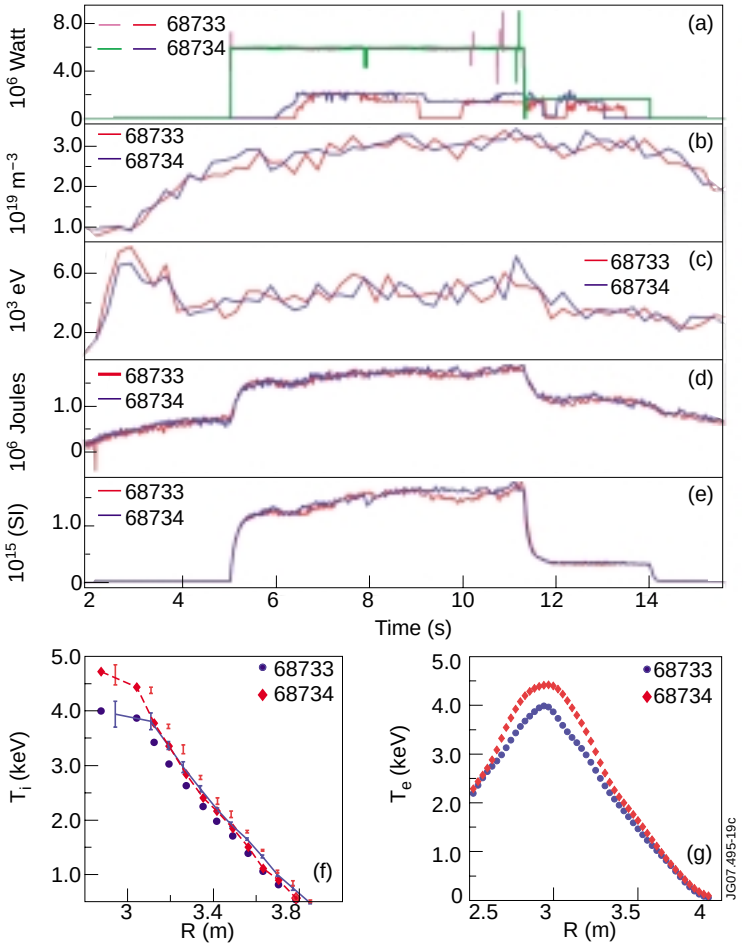

Figure 11: Comparison of B_o=3.3T and B_o=3.6T shots: (a) RF and NBI power, (b) central electron density, (c) central electron temperature, (d) diamagnetic energy and (e) neutron rate as a function of time. The bottom figures give the ion and electron temperature profiles at t=47s.

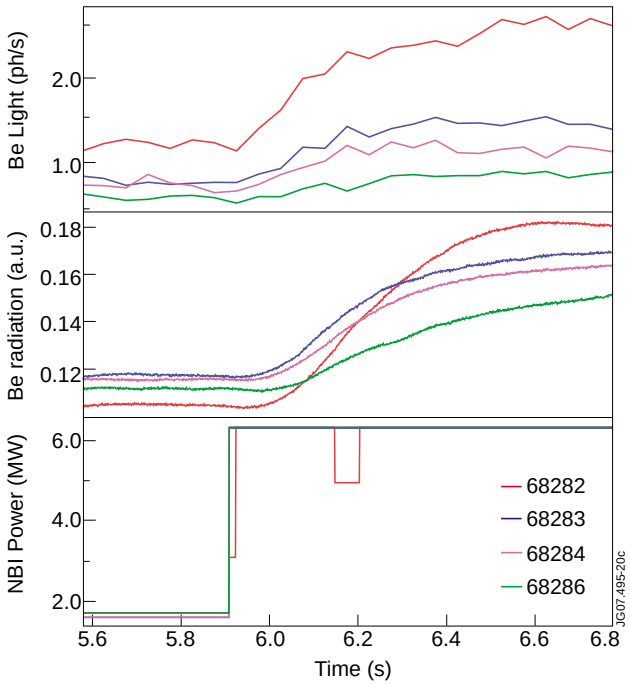

Figure 12: Beryllium light from visible spectroscopy (top), radiation from Be (middle) and neutral beam power (bottom) as a function of time for 4 subsequent shots just after Be evaporation.

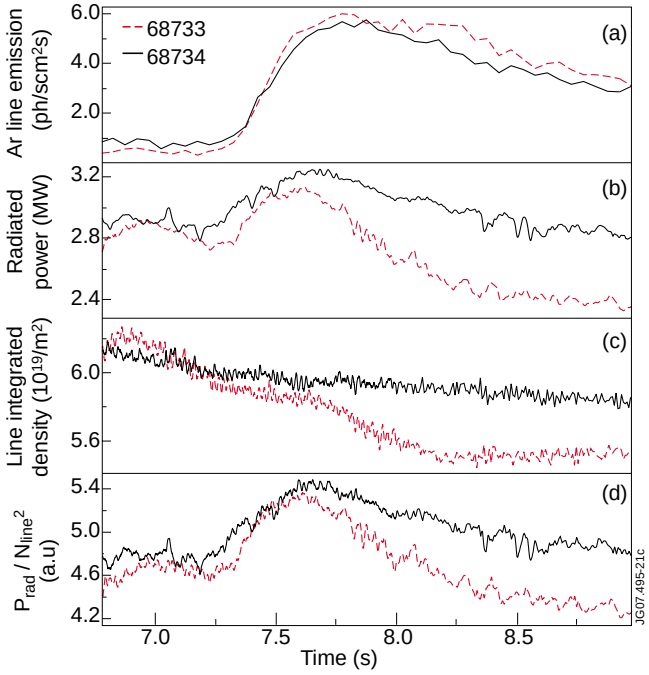

Figure 13: Visible spectroscopy emission and radiation due to Argon in the B_0 =3.3T bulk Deuterium central RF heating Pulse No: 68733 and the B_0 = 3.6T central impurity RF heating Pulse No: 68734: (a) Argon λ = 443nm line emission, (b) total radiated power, (c) line integrated central density, (d) P_{rad}/N_{line}^2.

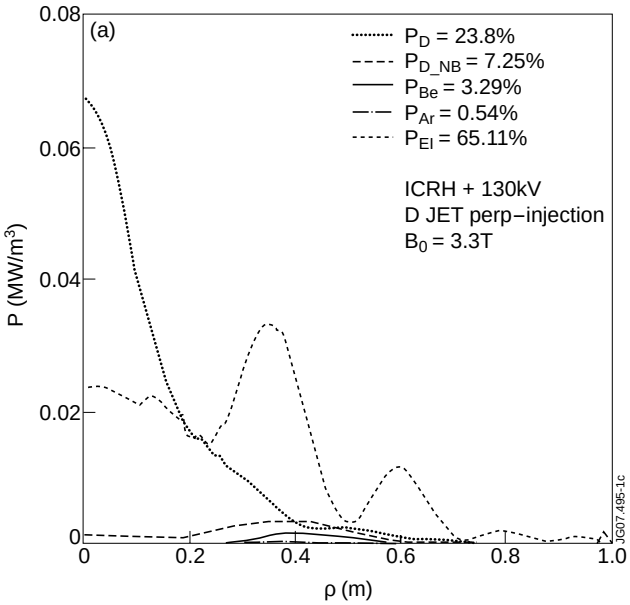

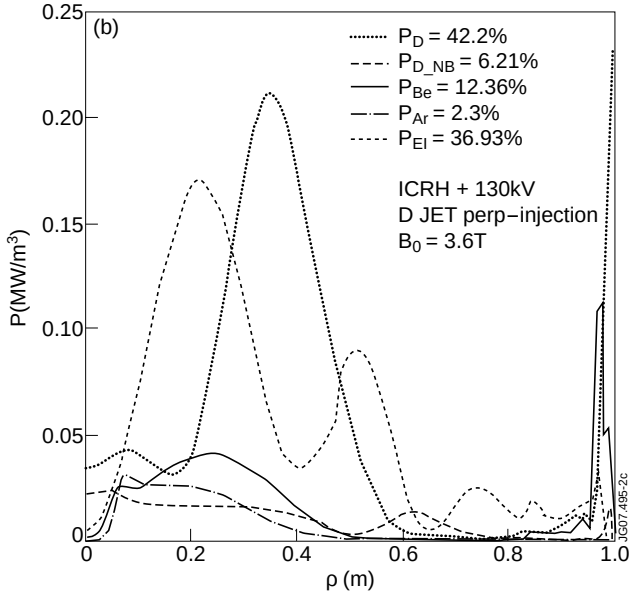

Figure 14: Distribution of the absorbed ICRH power simulated by the 3D PSTELION full wave code for JET experimental conditions with a fast D subpopulation with a concentration of (5%), a Be concentration of (1%) and an Ar concentration of 0.1%: (a) B_0 = 3.3T and (b) B_0 = 3.6T.